

Spectrum Analysis of Type IIb Supernova 1996cb

Jinsong Deng^{1,2}

*Research Center for the Early Universe, School of Science, University of Tokyo,
Bunkyo-ku, Tokyo 113-0033, Japan*

deng@astron.s.u-tokyo.ac.jp

Yulei Qiu and Jinyao Hu

Beijing Astronomical Observatory, Chaoyang District, Beijing 100012, P.R.China

qiuy1@nova.bao.ac.cn; hjy@class1.bao.ac.cn

ABSTRACT

We analyze a time series of optical spectra of SN 1993J-like supernova 1996cb, from 14 days before maximum to 86 days after that, with a parameterized supernova synthetic-spectrum code SYNOW. Detailed line identification are made through fitting the synthetic spectra to observed ones. The derived photospheric velocity, decreasing from 11,000 km s⁻¹ to 3,000 km s⁻¹, gives a rough estimate of the ratio of explosion kinetic energy to ejecta mass, i.e. $E/M_{\text{ej}} \sim 0.2 - 0.5 \times 10^{51}$ ergs/ $M_{\text{ej}}(M_{\odot})$. We find that the minimum velocity of hydrogen is $\sim 10,000$ km s⁻¹, which suggests a small hydrogen envelope mass of $\sim 0.02 - 0.1 M_{\text{ej}}$, or $0.1 - 0.2 M_{\odot}$ if E is assumed 1×10^{51} ergs. A possible Ni II absorption feature near 4000 Å is identified throughout the epochs studied here and is most likely produced by primordial nickel. Unambiguous Co II features emerge from 16 days after maximum onward, which suggests that freshly synthesized radioactive material has been mixed outward to a velocity of at least 7,000 km s⁻¹ as a result of hydrodynamical instabilities. Although our synthetic spectra show that the bulk of the blueshift of [O I] $\lambda 5577$ net emission, as large as ~ 70 Å at 9 days after maximum, is attributed to line blending, a still considerable residual ~ 20 Å remains till the late phase. It may be evidence of clumpy or large-scale asymmetric nature of oxygen emission region.

Subject headings: line: identification — radiative transfer — supernovae: individual (SN 1996cb) — supernovae: general

¹Department of Astronomy, School of Science, University of Tokyo, Bunkyo-ku, Tokyo 113-0033, Japan

²Beijing Astronomical Observatory, Chaoyang District, Beijing 100012, P.R.China

1. Introduction

SN 1996cb in NGC 3510 was first discovered by Aoki, Cho, and Toyama on 1996 December 15 (Nakano & Sumuto 1996), and independently by BAOSS on 1996 December 18 (Qiao et al. 1996). It was classified as a type IIb event due to spectral similarity to SN 1993J (Garbavich & Kirshner 1997). As reviewed by Filippenko (1997), this subclass of SNe II appear to be links between normal SNe II and SNe Ib. They show strong hydrogen Balmer lines near maximum brightness, then evolve with the disappearance of hydrogen features and the emergence of helium ones. Many days after maximum, their spectra are dominated by oxygen and calcium emission lines and hence resemble those of SNe Ib at the nebular phase. Their progenitors are usually thought to be massive stars, having lost most of their hydrogen envelopes either through stellar winds (e.g. Höflich, Langer, & Duschinger 1993), or more likely as the results of mass exchange with their companions (e.g. Nomoto et al. 1993; Podsiadlowski et al. 1993).

Very few type IIb events have been recognized to date. The first one is SN 1987K (Filippenko 1988), unfortunately whose proximity to the Sun made observations unavailable for a long period after maximum. Unlike it, the famous bright SN 1993J has been exposed to intensive observations and theoretical analysis (for a brief review, see Matheson et al. 2000a). For SNe 1997dd and 1998fa, it is only very recently that one and four spectra respectively were published (Matheson et al. 2001). No data of SNe 1996B (Wang & Wheeler 1996), 2000H (Benetti et al. 2000), 2001ad (Chornock, Modjaz, & Filippenko 2001), and 2001cf (Filippenko & Chornock 2001) have been released yet. Other proposed candidates, like SNe 1989O (Filippenko & Shields 1989) and 1999bv (Hill et al. 1999), were either distant or discovered at the late phase, with their classifications some uncertain.

Qiu et al. (1999) have published BVR_c light curves of SN 1996cb and its low-resolution optical spectra, obtained at Beijing Astronomical Observatory, from 14 days before maximum to 160 days after that. The light curves are very similar to those of SN 1993J, except that in SN 1996cb the initial peak due to shock breakout and the subsequent rapid decline have not been observed. The B light curve reached a maximum of 14.22 mag on 1997 January 2, which makes it the third brightest supernova discovered in 1996. By comparing its $B-V$ color curve with that of SN 1993J, they estimated the explosion date at 1996 December 12. They also described the observed spectral evolution in a brief way, while emphasizing the blueshift of He I $\lambda 5876$ and [O I] $\lambda 5577$ emission peaks. In SN 1993J, such a phenomenon for [O I] $\lambda 5577$ has been suggested being evidence of Rayleigh-Taylor instabilities at the He/C+O interface (Wang & Hu 1994).

It is important to analyze and model spectroscopic and photometric data of SN 1996cb, by far the only other well-observed SN 1993J-like supernova available for comprehensive

investigations. The results can be compared with those of SN 1993J. Numerous studies on the latter arrived at the conclusion that it is the explosion of a massive star with a $\sim 4 M_{\odot}$ helium core and a small He-rich hydrogen envelope of $\sim 0.1 - 0.9 M_{\odot}$ (Nomoto et al. 1993; Podsiadlowski et al. 1993; Shigeyama et al. 1994; Bartunov et al. 1994; Utrobin 1994; Woosley et al. 1994; Young, Baron, & Branch 1995, etc). These studies also have great influences on many aspects of our understanding of core-collapse supernovae, like the pre-supernova evolution in a binary system (e.g. Nomoto, Iwamoto, & Suzuki 1995), asymmetric nature of explosion (e.g. Wang et al. 2001), large-scale instability and mixing (e.g. Iwamoto et al. 1997), NLTE and non-thermal effects on spectrum formation (e.g. Houck & Frasson 1996), interaction of ejecta with circumstellar matter (e.g. Franson, Lundqvist, & Chevalier 1996), etc.

In this paper, we report our work on the synthesis of a spectra series of SN 1996cb from 1996 December 19 to 1997 March 28, spanning almost its whole photospheric stage. We use a parameterized supernova synthetic-spectrum code SYNOW. The method and parameters are described in §2. Our main goal is to establish line identifications, which are presented in §3 with our best fit synthetic spectra. Discussions on photospheric velocity, velocity and mass of hydrogen envelope, identifications of Ni II and Co II, blueshift of [O I] $\lambda 5577$, etc. are given in §4. The comparison with SN 1993J is mentioned wherever within reach. Our main conclusions are summarized in §5.

2. Spectrum Synthesis Procedure

To establish reliable line identifications, theoretical synthesis of supernova spectra is necessary. SYNOW is a parameterized supernova synthetic-spectrum code developed by Branch and collaborators and especially suitable for such a purpose (Branch 1980; Jeffery & Branch 1990; Fisher 2000). The current version of SYNOW uses 42 million line list of Kurucz (1993). It can treat the complicated line blending properly, but still retain a low cost of run-time. We know line blending is a great nuisance in the analysis of supernova spectra, which corresponds to nonlocal radiative coupling between different lines due to a large spatial gradient of velocity (Rybicki & Hummer 1978; Olson 1982). Numerical tests show that in the blending of a group of lines even features with large optical depth can be greatly suppressed and sometimes a single quasi-P Cygni profile, but unusually shaped, will be yielded (Jeffery & Branch 1990).

The basic physical assumptions and parameters adopted in SYNOW can be described as follows: The supernova ejecta is assumed spherically symmetric and with radial velocity $v \propto r$ at any radius r , namely in homologous expansion. The observed continuum is assumed

to arise out of a sharp photosphere and fitted by a blackbody one with temperature T_{bb} , while formation of spectral lines are treated as resonant scatterings of continuum photons above the photosphere in Sobolev approximation. No detailed ionization and excitation balance is considered; hence for each ion we choose the Sobolev optical depth, at the photosphere, of one reference line as a free parameter, with those of the others fixed by LTE assumption. The radial dependence of line optical depths is assumed to follow the density profile of ejecta, which is simplified to be either a power-law one, $\rho \propto \exp(-v/v_e)$, or an exponential one, $\rho \propto \exp(-v/v_e)$. The velocity of photosphere v_{ph} is an important fitting parameter.

In this work, we adopt an exponential density profile, $\rho \propto \exp(-v/v_e)$, with e-folding velocity $v_e = 2,000 \text{ km s}^{-1}$. To determine which ions should be invoked when computing a synthetic spectrum, we refer to line identifications for other Type II and Ib/c supernova, especially SN 1987A (e.g. Jeffery & Branch 1990) and SN 1993J (e.g. Matheson et al. 2000a). The systematic plots of LTE Sobolev line depths versus temperature, made by Hatano et al. (1999a), for some common supernova compositions are also useful. For each ion, the LTE excitation temperature T_{exc} is also a fitting parameter but bears little physical significance. We adapt T_{exc} in the range from 4,000 K to 12,000 K. We fix the outer edge of the line-forming region at $50,000 \text{ km s}^{-1}$. Sometimes we have to set for an ion a minimum velocity v_{min} , greater than v_{ph} , which shows that it is detached from the photosphere.

To make exact comparisons with synthetic spectra, the observed spectra should be transformed to the rest frame of the host galaxy and corrected for possible interstellar reddening. The recession velocity of NGC 3510 adopted here is $\sim 770 \text{ km s}^{-1}$ (Garbavich & Kirshner 1997). By comparing $B-V$ color curves, Qiu et al. (1999) argued that the color excess of SN 1996cb is 0.2 lower than that of SN 1993J. Although various values were found for the latter, the average seems ~ 0.2 (see Matheson et al. 2000b, and references therein). So we assume $E(B-V) \approx 0$ for SN 1996cb, which is consistent with the negligible Galactic component ~ 0.03 (Schlegel, Finkbeiner, & Davis 1998) and the absence of narrow Na I D absorption in a 50 \AA mm^{-1} dispersion spectrum taken on 1996 December 23 (Qiu et al. 1999).

3. Spectrum Evolution and Line Identification

For comparison with each observed spectrum, we have calculated many synthetic spectra with various values of the fitting parameters mentioned above. Our best fit synthetic ones are plotted as thick solid lines in Figures 1, 2, 3, and 4 together with observed ones (thin solid lines) in time sequence. The telluric O_2 absorptions of A-band ($\sim 7600 \text{ \AA}$) and B-band ($\sim 6850 \text{ \AA}$) are marked. We list in Table 1 the date of explosion, epoch, and best fit value of v_{ph} and T_{bb} . For each spectrum, two different epoch denotations are employed in this paper.

One is in days after the estimated explosion date, 1996 December 12; and the other is in days with respect to the date of B maximum, 1997 January 2, and always prefixed either a minus or a plus. For example, our first spectrum, taken on 1996 December 19, can be denoted as day 7 and -14 days respectively.

3.1. Day 7 to 20

The day 7 (-14 days) spectrum, shown in Figure 1, is similar to those of SN 1993J from 7 to 23 days after explosion, except the puzzling flat-topped characteristic of H_α in the latter (see Lewis et al. 1994; Prabhu et al. 1995; Baron et al. 1995; Finn et al. 1995, etc). P Cygni profiles of H_α , H_β , H_γ are distinct. Ca II H&K is strong, while the trough attributable to Ca II near-infrared triplet absorption is shallow. According to our synthetic spectrum, P Cygni features around 4400 Å and 4900 Å, and the very broad triangular one from 5000 Å and 5600 Å are produced by Fe II line blends. We can not reproduce the observed profile of H_α , which shows a net emission component with a blueshifted peak and a rather broad absorption base. To fit a prominent notch superimposed on the Ca II H&K emission, we introduce Ni II lines and blend them with H_δ . The strong P Cygni feature around 5800 Å is identified as He I λ 5876. The contribution from Na I D is supposed to be negligible because the temperature at such an early phase, $\sim 10,000$ K, is high enough to ionize all neutral sodium.

From day 10 (-11 days) to day 20 (-1 day), the top of H_α emission becomes flat and a notch gradually develops on it. To simulate this behavior, we must fix v_{\min}^{HI} at 10,500 km s⁻¹, while the photospheric velocity decreases from 10,000 km s⁻¹ to 8,000 km s⁻¹. It also requires a drop in the relative optical depth, $\tau_{\text{HI}}/\tau_{\text{HeI}}$, by one order from day 7 to day 20; and accordingly the notch is identified as He I λ 6678. In contrast to the first spectrum, here H_α profiles can be well fitted under our LTE purely resonant scattering assumption, which suggests that the hydrogen region is nearly recombined. All these show that the photosphere has receded through the H/He interface. In SN 1993J, this does not happen till 26 days after explosion (Matheson et al. 2000a, and references therein). A new feature at ~ 4100 Å, produced by Fe II, emerges from behind the weakened H_δ absorption due to de-blending. The “4000 Å” notch is also attributed much more to Ni II than to H_δ . Other line identifications are the same as those on day 7. However, to fit the observed spectra, here we must set $v_{\min} = 10,500$ km s⁻¹ for Fe II.

3.2. Day 24 to 46

Figure 2 shows the spectra from day 24 (+3 days) to day 46 (+25 days). The day 24 spectrum resemble those previous, but the constraint on v_{\min}^{FeII} is relaxed here and after. He I $\lambda 7065$ develops clear. Ni II helps somewhat to form a feature around 3700 \AA with Ca II, although the “ 4000 \AA ” notch that we attribute to Ni II and H_{δ} before disappears.

There are some noticeable changes in the day 30 spectrum: (1) The broad single “ $5000 - 5600 \text{ \AA}$ ” feature splits into three distinct bumps. The blueward two are most likely produced by Fe II lines in strongly blending. There are some controversy about the nature of the $\sim 5500 \text{ \AA}$ feature in spectra of SN 1993J, which can be traced back to as early as day 25 (Prabhu et al. 1995; Wang & Hu 1994). Following Wang & Hu (1994) and other authors, we suggest it as the blueshifted [O I] $\lambda 5577$ emission. By employing a low enough temperature of $T_{\text{exc}}^{\text{OI}} = 4,500 \text{ K}$, we can include forbidden lines [O I] $\lambda 5577$ and $\lambda \lambda 6300, 6364$ in our synthetic spectra, without causing an unreasonably strong O I $\lambda 7773$. (2) The deep notch at 4370 \AA and an inconspicuous dip on the top of He I $\lambda 5876$ emission can be fitted by Ba II $\lambda 6142$ and $\lambda 4554$ respectively, if $v_{\min}^{\text{BaII}} = 13,000 \text{ km s}^{-1}$ is set. The dip just blueward to H_{β} is identified as $\lambda \lambda 4738, 4744$ absorption of C II detached at $v_{\min} = 9,800 \text{ km s}^{-1}$. We attribute the feature located at 4290 \AA to V I absorption. (3) Ca II H&K emission becomes weak and shows an unusual triangular profile centered at 4006 \AA . The redward decline can be well reproduced. But the fit to the blueward incline, which is remarkably redshifted, can only be partially improved by including Ni II absorption.

Day 37 and day 46 spectra are dominated by He I $\lambda 5876$ (blended with Na I D), $\lambda 6678$, $\lambda 7065$, and $\lambda 7281$ P Cygni lines in the red. He I also contributes a lot to absorptions at 4380 \AA , 4820 \AA , and 4900 \AA . A distinct notch appears at 4080 \AA is identified as Co II feature through spectral synthesis. If Co II is removed, there will be obvious discrepancies also in other regions between model spectra and observations. We noticed there is an absorption feature near 4100 \AA in the spectra of SN 1993J from day 56 to 109 (Matheson et al. 2000a; Lewis et al. 1994; Swartz et al. 1993b) but unfortunately without identification. Ni II $\sim 4000 \text{ \AA}$ feature, with a minor contribution from He I, lies just redward to Ca II H&K absorption, which becomes rather weak now. We must decrease the optical depth of Fe II to explain the nearly absence of Fe II $\lambda 5169$. From day 46 onward, Fe I is introduced to lower the flux bluer than 4500 \AA to the observed level, and also helps to form the basin-like shape between 5000 \AA and 5500 \AA . Ba II and V I features seen in day 30 spectrum have completely disappeared.

3.3. Day 51 to 107

Figures 3 and 4 show the spectra from day 51 (+30 days) to day 107 (+86 days). H Balmer lines continue to weaken fast, consequently the spectra resemble those of Type Ib more and more. Although a narrow H_α absorption and an inconspicuous H_β feature remain till day 107, they nearly vanish in the April 4 spectrum (day 114) of Qiu et al. (1999) and April 16 spectrum of Matheson et al. (2001). He I line intensity culminates around day 55, and then begins to decay, especially that of $\lambda 6678$. Because of this and also of the decrease of photospheric velocity, telluric O_2 B-band ($\sim 6850 \text{ \AA}$) reappearances and contributes to a somewhat misleading flat-bottomed profile.

Forbidden emissions like [Ca II] $\lambda\lambda 7291, 7324$, near-infrared triplet and narrow Mg I] $\lambda 4571$ develop in this period, which designates a transition to the nebular phase. In accordance, the light curve of SN 1996cb enters its tail around day 50 (Qiu et al. 1999). We can not produce these nebular features with SYNOW due to their non-resonant-scattering nature. [O I] $\lambda 5577$ does not strengthen much throughout this epoch, while the gradually standing-out of [O I] $\lambda\lambda 6300, 6364$ emission is attributed more to the weakening of H_α absorption than to the change of oxygen abundance. There seems some O I $\lambda 7773$ emission, although the possible absorption is greatly contaminated by telluric O_2 A-band.

Fe II is removed from our synthetic spectra since day 51 and is introduced again since day 87, in order to simulate the evolution of Fe II $\lambda 5169$. We fail to fit the excessive intensity of supposed He I/Fe II P Cygni feature around 5000 \AA . NLTE effects may account for it. The excellent fit to the observed multi-peak shape between $3800 - 4400 \text{ \AA}$ seems striking, considering numerous transitions of Fe I, Fe II, Co II, and Ni II in operation and complicated blending effects between them. That is to say, our introduction of Ni II, Co II, and Fe I is somewhat valid. Note the Fe I feature just redward to H_γ in Figure 3 and other Fe I features in Figure 4.

Overall, line identifications change little from day 37 to day 107, which means that there is no evident composition stratification in the velocity range from $7,000 \text{ km s}^{-1}$ to $3,000 \text{ km s}^{-1}$. The spectra are fully dominated by [O I] and [Ca II] nebular emissions since 1997 April (Qiu et al. 1999; Matheson et al. 2001), when the photosphere has most likely receded into the oxygen core. Analysis of subsequent nebular spectra goes beyond the ability of SYNOW.

4. Discussion

4.1. Evolution of Photospheric Velocity

The most reliable parameter fixed by the spectral synthesis with SYNOW is the photospheric velocity. Absorption minima of some weak lines, e.g. Fe II $\lambda 5018$, $\lambda 5169$, and H_γ , are often regarded as good tracers of v_{ph} in Type II (e.g. Eastman & Kirshner 1989; Duschinger et al. 1995). However, they more or less blend with others and sometimes can not be identified correctly. With SYNOW, information not only on minima positions but also on profiles, and of as many as possible features, can be used to determine v_{ph} in a consistent way, while line blending and optical depth effects have been taken into account.

We plot in Figure 5 the the evolution of photospheric velocity of SN 1996cb, derived from our spectral synthesis. The error is estimated less than $\pm 500 \text{ km s}^{-1}$. We can see that v_{ph} declines monotonically from $11,000 \text{ km s}^{-1}$ on day 7 to $3,000 \text{ km s}^{-1}$ on day 107 days. For comparison, photospheric velocities of SN 1993J measured in absorption minimum of Fe II $\lambda 5018$ (Prabhu et al. 1995; Baron et al. 1995) are plotted in the same figure. They are similar to each other on the whole, while the difference at late phase may demonstrate that Fe II $\lambda 5018$ does not follow v_{ph} very well (note that measurement of the same line in our SN 1996cb spectra also gives a value $\gtrsim 6,000 \text{ km s}^{-1}$ after day 80).

For given ejecta mass M_{ej} and explosion kinetic energy E , we know v_{ph} roughly scales as $(E/M_{\text{ej}})^{1/2}$. The exact relationship depends on the specific hydrodynamical structure of supernova ejecta. Considering the exponential density profile adopted for our spectral synthesis

$$\rho = \rho_0 \cdot \exp(-v/v_e) , \quad (1)$$

where ρ_0 is the central density and v_e is the e-folding velocity, one immediately gets

$$E = 6M_{\text{ej}}v_e^2 . \quad (2)$$

Defining $\bar{\kappa}$ as the average opacity above the photosphere, we find that the evolution of photospheric velocity can be approximately expressed as

$$v_{\text{ph}} \approx -v_e \ln \left[10^{-6} \frac{\tau_{\text{ph}}}{\bar{\kappa}} v_{e,3}^2 \left(\frac{M_\odot}{M_{\text{ej}}} \right) \right] - 2v_e \ln t_d , \quad (3)$$

where $\tau_{\text{ph}} \approx 1$ or $2/3$ is the optical depth at the photosphere, $v_{e,3}$ is v_e in 10^3 km s^{-1} and t_d is time in days since explosion. Fitting of data shown in Figure 5 by the above equation gives $v_e \approx 1,400 \text{ km s}^{-1}$, a little smaller than our trial value of $2,000 \text{ km s}^{-1}$ for spectral synthesis, and

$$M_{\text{ej}} \approx 4M_\odot \cdot \tau_{\text{ph}} \cdot \left(\frac{\bar{\kappa}}{0.07} \right) , \quad (4)$$

$$E \approx 0.9 \times 10^{51} \text{ ergs} \cdot \left(\frac{M_{\text{ej}}}{4 M_{\odot}} \right). \quad (5)$$

However, the actual density profile may be far from an exponential one (In fact, $v_{\text{ph}}(t)$ shown in Figure 5 can also be well fitted by assuming a power-law density profile). Referring to the 4H89 model for SN 1993J presented by Shigeyama et al. (1994, Fig. 2), in which the density distribution approximates to $\rho \propto v^{-6}$ between 24,000 – 5,500 km s⁻¹ and remains roughly constant below 5,500 km s⁻¹, we then assume in SN 1996cb

$$\rho = \begin{cases} \rho_c \cdot \left(\frac{v}{v_c}\right)^{-n}, & v > v_c; \\ \rho_c, & v \leq v_c. \end{cases} \quad (6)$$

Integrating ρ and ρv^2 over velocity, we get

$$E = \frac{3(n-3)}{5(n-5)} v_{c,4}^2 \left(\frac{M_{\text{ej}}}{M_{\odot}} \right) \times 10^{51} \text{ ergs}, \quad (7)$$

where $v_{c,4}$ is the characteristic velocity in 10⁴ km s⁻¹. We find the evolution of photospheric velocity can be described as

$$v_{\text{ph}} = \begin{cases} v_c \cdot \left(\frac{t}{t_c}\right)^{-2/(n-1)}, & t > t_c; \\ \frac{n \cdot v_c}{n-1} - \frac{v_c}{n-1} \cdot \left(\frac{t}{t_c}\right)^2, & t \leq t_c, \end{cases} \quad (8)$$

which shows that (t_c, v_c) is a inflection point. If we suppose the bump from day 30 to 50 in Figure 5 is more or less relevant to the so-called inflection point, we then estimate v_c at $\sim 7,000 - 5,500$ km s⁻¹. By fitting $v_{\text{ph}}(t < t_c)$, we find $n \approx 7.4$ for $v_c = 7,000$ km s⁻¹ and $n \approx 7.2$ for $v_c = 5,500$ km s⁻¹. Substituting these values into equation (8), one finally obtains

$$E \approx 1 - 1.6 \times 10^{51} \text{ ergs} \cdot \left(\frac{M_{\text{ej}}}{3 M_{\odot}} \right). \quad (9)$$

We know the typical value of explosion kinetic energy for core-collapse supernova is 1×10^{51} ergs, accordingly equations (9) and (5) suggest that ejecta mass of SN 1996cb possibly lies in the range of 2 – 5 M_{\odot} , similar to those of SN 1993J and Type Ib (Shigeyama et al. 1990). More reasonable constraints on E and M_{ej} can be made by exploding a realistic progenitor model and reproduce both light curves and $v_{\text{ph}}(t)$ shown in Figure 5.

4.2. He-rich Hydrogen Envelope with High Velocity

It is crucial to determine the distribution and mass of hydrogen in Type IIb supernovae for the understanding of their unusual pre-explosion evolution. For SN 1993J, most authors

doing hydrodynamical calculations inferred a low-mass He-rich hydrogen envelope of $\sim 0.1 - 1 M_{\odot}$ (Nomoto et al. 1993; Podsiadlowski et al. 1993; Shigeyama et al. 1994; Bartunov et al. 1994; Utrobin 1994; Woosley et al. 1994; Young, Baron, & Branch 1995, etc), which is consistent with NLTE modeling of photospheric spectra (Swartz et al. 1993b; Zhang & Wang 1996). By analyzing its H_{α} emission in nebular spectra, Patat, Chugai, & Mazzali (1995) concluded that ionized hydrogen is distributed between $7,500 - 11,400 \text{ km s}^{-1}$ with density maximum at $8,900 - 9,300 \text{ km s}^{-1}$. Utrobin (1996) arrived at a very similar conclusion in his light curve study including nonthermal ionization. Applying a sophisticated NLTE code to nebular spectra, Houck & Frasson (1996) argued that the bulk of the preferred H/He envelope mass, $0.2 - 0.4 M_{\odot}$, lies between $8,500 - 10,000 \text{ km s}^{-1}$, and ruled out the presence of more than $0.02 M_{\odot}$ of hydrogen above or below this range.

As described above, to fit photospheric spectra of SN 1996cb, the line forming region of hydrogen is required to be detached from the photosphere after day 10. The adopted value of parameter $v_{\text{min}}^{\text{HI}}$ only varies in a very narrow range, $9,500 - 10,500 \text{ km s}^{-1}$. It is about $1,000 \text{ km s}^{-1}$ smaller than the absorption velocity of H_{α} till day 46; but after that it approaches the latter. In comparison, absorption velocity of H_{α} and H_{β} in SN 1993J, considerably declining during the first 50 days, stop around $9,500 \text{ km s}^{-1}$ and $8,500 \text{ km s}^{-1}$ respectively from day 50 to day 70 (Barbon et al. 1995). After day 100, as H_{α} absorption is no longer optical thick, the velocity reaches $8,500 \text{ km s}^{-1}$, i.e. the minimum velocity of hydrogen envelope derived by Houck & Frasson (1996). Accordingly, we can say that the inner boundary of hydrogen envelope of SN 1996cb exists at $9,500 - 10,500 \text{ km s}^{-1}$, higher than of SN 1993J.

In the explosion of a Type IIb supernova, due to the supposed low mass of hydrogen envelope, the deceleration of shock wave at the H/He interface and consequent Rayleigh-Taylor instability is rather weak (Iwamoto et al. 1997). As a result, the minimum velocity of hydrogen envelope depends mainly on its mass, M_{env} . Thus one can expect an even smaller M_{env} for SN 1996cb than for SN 1993J. Considering an ejecta with the exponential density profile given by equation (1), the mass above $v_{\text{min}}^{\text{H}} \approx 9,500 - 10,500 \text{ km s}^{-1}$, i.e. M_{env} , is

$$M_{\text{env}} = \left[\frac{1}{2}f^2 + f + 1 \right] e^{-f} \cdot M_{\text{ej}} \quad (10)$$

$$\approx 0.02 - 0.04 M_{\text{ej}} , \quad (11)$$

where $f \equiv v_{\text{min}}^{\text{H}}/v_e$. And for the density profile given by equation (7), M_{env} is

$$M_{\text{env}} = \frac{3}{n} \cdot \left(\frac{v_c}{v_{\text{min}}^{\text{H}}} \right)^{n-3} \cdot M_{\text{ej}} \quad (12)$$

$$\approx \begin{cases} 0.07 - 0.1 M_{\text{ej}} , & v_{c,4} = 0.7 ; \\ 0.03 - 0.04 M_{\text{ej}} , & v_{c,4} = 0.55 . \end{cases} \quad (13)$$

Combining equations (11) and (13) with equations (5) and (9) respectively, and assuming $E \approx 1 \times 10^{51}$ ergs, we find the mass of hydrogen envelope of SN 1996cb is $M_{\text{env}} \sim 0.1\text{--}0.2 M_{\odot}$, near the low end among different estimated values for SN 1993J.

As argued above, the photosphere in SN 1996cb recedes through the H/He interface around day 10, much earlier than in SN 1993J, say day 26. This could be explained by the smallness of M_{env} compared with SN 1993J. It is well known that, opacity in the hydrogen envelope is dominated by free electron scattering at the early phase. Then the optical depth at the the H/He interface at time t after explosion roughly scales as

$$\tau \sim n_e \sigma_T \ell , \quad (14)$$

where $\ell \sim v_{\text{min}}^{\text{H}} t$ is the characteristic length in the hydrogen envelope, n_e is the characteristic electron density and σ_T the Thompson scattering cross section. It is nonthermal ionization by relativistic electrons that prevents the hydrogen envelope from being completely recombined after the initial rapid cooling stage (Wheeler & Filippenko 1996; Utrobin 1996). Adopting a simple balance between collisional recombination and nonthermal ionization,

$$\alpha n_e N^+ \sim \Gamma N , \quad (15)$$

and neglecting any variation among the effective collisional recombination coefficient α and the effective nonthermal ionization coefficient Γ , one gets

$$n_e \sim N^+ \propto \sqrt{N} \sim \sqrt{\frac{M_{\text{env}}}{\ell^3}} . \quad (16)$$

When the photosphere arrives at the H/He interface, i.e. $\tau \approx 1$, substituting of equation (16) into equation (14) gives

$$t \propto \frac{M_{\text{env}}}{v_{\text{min}}^{\text{H}}} . \quad (17)$$

It is obvious that this equation is in agreement with the comparison between SN 1996cb and SN 1993J.

Helium abundance Y in the so-called hydrogen envelope should be very high, which is suggested by strong He I $\lambda 5876$ feature in the spectrum of SN 1996cb on day 7, when the photosphere still stays in the envelope. We know the line Sobolev optical depth is

$$\tau \approx 0.23 f \cdot \lambda(\mu\text{m}) \cdot N_{\ell}(\text{cm}^{-3}) \cdot t_{\text{d}} , \quad (18)$$

where f is the oscillator strength, λ is the rest wavelength, N_{ℓ} is the atomic number density in the lower state, t_{d} is time in days after explosion and the term for induced emission is neglected. Under the LTE assumption, the adopted optical depths of reference lines and

excitation temperatures for H I and He I give $N_{\text{HI}} \sim 10^6 \text{ cm}^{-3}$ and $N_{\text{HeI}} \sim 10^9 \text{ cm}^{-3}$, respectively, at the photosphere on day 7, while the electron density required for continuum optical depth is $n_e \sim 10^{10} \text{ cm}^{-3}$. These values, although rather uncertain, may show both that the helium abundance is high and a large fraction of H and He are ionized. Through NLTE modeling of early spectra, Baron, Hauschildt, & Branch (1994) found $Y \approx 0.8$ for the envelope of SN 1993J.

A He-rich hydrogen envelope is the natural result of pre-supernova evolution with large mass loss (Saio, Kato, & Nomoto 1988; Woosley et al. 1994). For given M_{core} , M_{env} , Y and surface radius R_0 , a hydrostatic and thermal equilibrium H/He envelope can be constructed upon the helium core (Saio, Kato, & Nomoto 1988). Since the initial adiabatic cooling stage in SN 1996cb ends before the discovery, i.e. day 3, much earlier than in SN 1993J, i.e. day 9, R_0 of the progenitor of SN 1996cb should be smaller than that of SN 1993J ($\sim 400 R_{\odot}$, Iwamoto et al. 1997). A solution of $(M_{\text{core}}, M_{\text{env}}, Y, R_0)$ that can fit both the light curve and the day 7 spectrum will discriminate the pre-explosion paths of SN 1996cb and SN 1993J.

We note before the excessive emission of H_{α} in day 7 spectrum and its blueshifted peak can not be fitted with SYNOW. As in the atmospheres of normal Type II, it can be attributed to NLTE effects and the significant extension of the line forming region (e.g. Duschinger et al. 1995; Eastman, Schmidt, & Kirshner 1996). Collisional recombination of H^+ to $n \geq 3$ levels and subsequent cascade transitions may also contribute. Zhang et al. (1995) introduced a smooth but tenuous outer layer of the envelope to model the unusually broad H_{α} absorption profile in early spectra of SN 1993J, which also appears in day 7 spectrum of SN 1996cb but is less prominent and hence suggests a somewhat different density profile for the outer layer.

4.3. Identifications of Ni II and Co II Lines

We find that Ni II significantly contributes to an absorption feature near $\sim 4000 \text{ \AA}$, i.e. adjacent to Ca II H&K. These lines, mostly Ni II $\lambda\lambda 4016, 4067$, have been identified unambiguously in photospheric spectra of some Type Ia (e.g. Mazzali et al. 1997; Hatano et al. 1999b). This is not unexpected since in thermonuclear explosions of white dwarfs Ni is synthesized in large abundance and distributed outward to rather high velocity. As to core-collapse supernovae, Deng et al. (2000) introduced Ni II to account for the “3930 \AA absorption” in their September 14 spectrum of Type Ib SN 1999dn, while Mazzali, Iwamoto, & Nomoto (2000) found that Ni II and Co II lines help to form the unusual spectra of Type Ic hypernova SN 1997ef.

Ni identified in SN 1996cb is probably primordially originated. For core-collapse su-

pernovae, typically $\sim 0.1 M_{\odot}$ newborn ^{56}Ni is ejected but, if without mixing, buried in the innermost layer of the ejecta. On the other hand, artificial large-scale outward mixing of ^{56}Ni plays an important role in reproducing observed light curves (e.g. Blinnikov et al. 2000) and spectra (e.g. Lucy 1991) with one-dimensional models. 2D and 3D hydrodynamical numerical simulations demonstrated that large-scale mixing can be induced by nonlinear growth of Rayleigh-Taylor instabilities and can transport ^{56}Ni to $\lesssim 2000 \text{ km s}^{-1}$ for Type II SNe (e.g. Kifonidis et al. 2000) and to $\lesssim 7000 \text{ km s}^{-1}$ for Type Ib/Iib SNe (e.g. Hachisu et al. 1991; Iwamoto et al. 1997). Accordingly, Ni II 4000 Å feature identified in SN 1996cb as early as day 7, when the photosphere is well in the hydrogen envelope and with a velocity as high as $11,000 \text{ km s}^{-1}$, is unlikely to be produced by newborn ^{56}Ni . Additional evidence comes from the fact that the Ni II feature remains discernible far beyond the half life of ^{56}Ni , ~ 6 days.

An alternative explanation for high velocity Ni II is asymmetry. Nagataki, Shimizu, & Sato (1998) and Maeda et al. (2000) have calculated nucleosynthesis for axisymmetric supernova explosions and concluded that ^{56}Ni can be accelerated to very high velocities roughly along the axial direction. A bipolar scenario of explosion for Type IIb supernova is also the suggestion of Wang et al. (2001), who noticed the strikingly similarity of spectropolarimetry between SN 1993J and SN 1996cb.

The identification of Co II in SN 1996cb seems more reliable than that of Ni II. Distinct Co II features emerged in the blue part of spectra since day 37, when the photosphere velocity declined to $7,000 \text{ km s}^{-1}$. This can be regarded as direct spectral evidence of large-scale outward mixing of radioactive elements in explosion. We mentioned earlier that similar but less distinct Co II features may occur in SN 1993J after day 56, when the photospheric velocity is lower than $6,000 \text{ km s}^{-1}$. This is consistent with the results of light curve modeling (Iwamoto et al. 1997) and NLTE analysis of nebular spectra (Houck & Frasson 1996), that maximum velocity of ^{56}Ni for SN 1993J most likely lies in the range of $\sim 4,000 - 6,000 \text{ km s}^{-1}$. As shown by Hachisu et al. (1991) and Iwamoto et al. (1997), the extent of ^{56}Ni mixing provides a constraint on the mass of helium core of the progenitor, M_{α} , that more extensive mixing is induced by R-T instabilities for smaller M_{α} , and that $v_{\text{max}}^{\text{Ni}} \sim 6,000 \text{ km s}^{-1}$ for $M_{\alpha} = 3.3 M_{\odot}$ and $v_{\text{max}}^{\text{Ni}} \sim 3,000 \text{ km s}^{-1}$ for $M_{\alpha} = 4 M_{\odot}$. Accordingly, the mass of helium core of SN 1996cb may be $\lesssim 3.3 M_{\odot}$, i.e. a little smaller than that of SN 1993J. The more extensive mixing of ^{56}Ni also helps to explain the earlier start of the radioactive heating stage in the light curve of SN 1996cb than in that of SN 1993J.

4.4. Blueshift of [O I] $\lambda 5577$ Emission Peak

We identify the distinct ~ 5500 Å bump, in photospheric spectra of SN 1996cb from day 30 onwards, as blueshifted [O I] $\lambda 5577$ emission. The appearance of this line at such early phase was first mentioned by Harkness et al. (1987) in Type Ib SNe 1983N and 1984L. But Filippenko, Porter, & Sargent (1990) argued that spectral synthesis is required to make a reliable identification, when analyzing spectra of Type Ic SN 1987M (see also Swartz et al. 1993a). Wang & Hu (1994) found that in SN 1993J this feature can be traced back to as early as day 27 and also noticed its apparent blueshift, which they attributed to a clumpy nature of ejecta near the He/C+O interface. Filippenko, Matheson, & Barth (1993) mentioned that the blueshift of emission lines is just a consequence of viewing primarily the near side of the optically thick ejecta. Spyromilio (1994) compared peak wavelengths of [O I] lines and Mg I] 4571 with those of permitted lines and proposed a large-scale asymmetric distribution of radioactive material for SN 1993J. However, through modeling nebular spectra of SN 1993J, Houck & Frasson (1996) concluded that the bulk of the blueshift of [O I] lines can be explained by line blending effects. Blueshift of the order of $1,000 \text{ km s}^{-1}$ is also observed for emission lines at late phases of Type Ib SN 1996N (Sollerman, Leibundgut, & Spyromilio 1998).

To study the effect of line blending on the blueshift of [O I] $\lambda 5577$ at photospheric phases, we try to include [O I] $\lambda 5577$ and $\lambda\lambda 6300, 6364$ into our synthetic spectra by setting an excitation temperature as low as $4,500 \text{ K}$. This technique is roughly valid because the emission peak of a pure resonant scattering line, in a spherically symmetric and homologous expanding atmosphere, exists at the rest wavelength if without blending (Jeffery & Branch 1990), although in fact [O I] net emissions is mainly produced via other processes, like electron collisional excitation. Peak wavelength of [O I] $\lambda 5577$ both in observed spectra and in our best fit synthetic ones are plotted in Figure 6. These values are simply measured by hand, for the accuracy is not crucial here. On day 97 and 107, some features or noise develop on the top of [O I] $\lambda 5577$, so we introduce error bars to describe the possible large uncertainty.

Figure 6 shows that the observed blueshift declines steadily from ~ 70 Å on day 30 to ~ 20 Å on day 107. This trend is reproduced in the rough by our synthetic data, which can only be interpreted as the variation of blending effects because neither asymmetry nor clumping is involved in our spectral synthesis. On the other hand, a blueshift of ~ 20 Å of the observed peak wavelength to the synthetic one remains throughout the period covered by Figure 6, while the latter approaches to 5577 Å finally. Furthermore, if we check the nebular spectra in April or May of 1997 (Qiu et al. 1999; Matheson et al. 2001), we can find that [O I] $\lambda 5577$ is still blueshifted by ~ 20 Å.

The bulk of the blueshift of [O I] $\lambda 5577$ Å at photospheric phases in SN 1996cb can be accounted for by line blending, but the rest of ~ 20 Å, i.e. ~ 1000 km s $^{-1}$, still demands an explanation. (1) The clumping model of Wang & Hu (1994) seems less likely because the [O I] emission peak never return to the rest wavelength, even after the photosphere has receded deep into the oxygen core. However, a photospheric spectrum code which can manage a clumpy ejecta well, e.g. by using the Monte Carlo technique, is required to clarify if clumping can affect the peak wavelength of line emission more or less. (2) At photospheric phases, the occultation of the main receding part of emission line forming region by the photosphere will also contribute somewhat to the residual blueshift, especially if NLTE effects can remarkably populate the upper level of [O I] $\lambda 5577$ transition, $2p^4(^1S)$, well above the photosphere. (3) Houck & Frasson (1996) and Sollerman, Leibundgut, & Spyromilio (1998) found the blueshift of O I $\lambda 777$ in nebular spectra of SN 1993J, $\lesssim 500$ km s $^{-1}$, and of SN 1996N, ~ 1000 km s $^{-1}$, respectively. Since this line is probably free of strong blending, they suggested that it is indicative of real asymmetry, possibly related to large-scale mixing.

In photospheric spectra of SN 1996cb, O I $\lambda 7773$ is inconspicuous and contaminated by telluric absorption. [O I] $\lambda\lambda 6300, 6364$ photons are strongly blended with each other and scattered by H $_{\alpha}$ transition. Therefore the measurement of peak wavelengths of these lines is of no significance. On the other hand, the distinct Mg I] $\lambda 4571$ narrow emission in our day 51 and 87 spectra peaks at ~ 4592 Å, i.e. apparently redshifted. Does features of Mg I] and [O I] come from different asymmetry and hence hint different mixing behavior? The peak wavelength of prominent [Ca II] $\lambda\lambda 7291, 7324$ emission evolves from 7304 Å on day 51 to 7324 Å on day 107. Considering the blending with He I $\lambda 7281$ in the beginning, it is just to say that no blueshift exists (cf. SN 1996N Sollerman, Leibundgut, & Spyromilio 1998). This is consistent with the conclusion for SN 1987A that calcium is most likely primordial and much less clumpy than oxygen (Li & McCray 1992, 1993).

Is the electron density in SN 1996cb as early as day 30 low enough to favor the emission of oxygen forbidden lines? We know the critical electron density for [O I] $\lambda 5577$ forbidden transition is

$$N_e^{\text{crit}} = \frac{g_u A_{ul}}{8.6 \times 10^{-6} T_e^{-1/2} \Omega_{ul}(T_e)}, \quad (19)$$

where the statistical weight $g_u = 5$, the spontaneous radiative transition rate $A_{ul} \approx 1.22$ s $^{-1}$, T_e is the electron temperature, and the effective collision strengths Ω_{ul} is found from Bhatia & Kastner (1995). The calculated N_e^{crit} is insensitive to T_e and, when $T_e \sim 5,000$ K, $N_e^{\text{crit}} \sim 7 \times 10^8$ cm $^{-3}$. Assuming pure Thompson scattering continuum optical depth, we can express the electron density at the photosphere as

$$n_e^{\text{ph}} = \frac{\tau_{\text{ph}}}{\sigma_e v_e t} \approx \frac{2 \times 10^{11} \text{ cm}^{-3}}{v_{e,3} t_d} \quad (20)$$

for the density profile defined by equation (1), and as

$$n_e^{\text{ph}} = \frac{(n-1)\tau_{\text{ph}}}{\sigma_e v_{\text{ph}} t} \approx \frac{(n-1) \cdot 2 \times 10^{11} \text{ cm}^{-3}}{v_{\text{ph},3} t_{\text{d}}} \quad (21)$$

for the density profile defined by equation (6). Both equations give $N_e^{\text{ph}} \sim 5 \times 10^9 \text{ cm}^{-3}$ on day 30, which does not differ much from N_e^{crit} for [O I] $\lambda 5577$. We note that Swartz et al. (1993b) exploit a low-density outer layer in high velocity, say $12,000 \text{ km s}^{-1}$, to fit oxygen features in photospheric spectra of SN 1993J. This assumption seems both unnecessary and unreasonable.

Qiu et al. (1999) also noticed the apparent blueshift of He I $\lambda 5876$ emission peak at very early phases and its subsequent recession to the rest wavelength in SN 1996cb. They claimed it as evidence of prominent Rayleigh-Taylor instabilities at the H/He interface. However, according to two-dimensional simulations, R-T instabilities must be weak at the H/He interface of Type IIb because of small envelope mass (e.g. Iwamoto et al. 1997). We plot in Figure 7 peak wavelength of He I $\lambda 5876$ both in observed spectra and in our best fit synthetic ones. The observed values can be reproduced very well by our synthetic spectra. Obviously, the blueshift of He I $\lambda 5876$ emission peak is superficial and can be attributed to the strong blending effects with H_α . After day 37, He I $\lambda 5876$ emission peak is redshifted into the range of $5876 - 5893 \text{ \AA}$, which shows that contribution from Na I D becomes noticeable.

4.5. Some Ambiguous Identifications

Three distinct notches at 4290 \AA , 4370 \AA , and 4610 \AA appears on day 30 spectrum and have been identified as V I absorption, Ba II $\lambda 4554$, and C II $\lambda\lambda 4738, 4744$, respectively. With some caution, they can be traced back to day 24 spectrum. However, we must note here that these identifications are rather ambiguous.

First, the ionization potential of V I, only 6.7 eV , seems too small to prevent it from being largely ionized. Therefore the 4290 \AA feature is more likely attributed to Ti II absorption, just like in SN 1987A (Jeffery & Branch 1990), Type Ic SN 1994I (Millard et al. 1999), and Type Ic hypernova SN 1997ef (Mazzali, Iwamoto, & Nomoto 2000), etc. However, with Ti II we can not produce the required notch but lower the flat top of H_γ uniformly, unless we set a strong constraint on the line forming region, say $v_{\text{max}}^{\text{TiII}} \lesssim 10,000 \text{ km s}^{-1}$. This does not necessarily rule out this ion, because many Ti II lines in strongly blending is involved and NLTE effects if existed will complicate the case greatly.

At first sight, the identification of Ba II $\lambda 4554$ is more or less credible, since the observed feature is prominent and another absorption feature can be fitted by Ba II $\lambda 6142$ consistently.

But the required minimum velocity of the line forming region, $v_{\min}^{\text{BaII}} = 13,000 \text{ km s}^{-1}$, is far from explicable. How can the barium material obtain significant resonant scattering optical depth when the photosphere is 6000 km s^{-1} below, considering that both the ejecta and the radiation field have been greatly diluted compared with the photosphere? Is it produced by a mass of dense barium cloudy which run into our line of sight from day 24 to day 37, say by the rotation of supernova? But the required rotational velocity is $> 10^3 \text{ km s}^{-1}$ and hence impossible. Matheson et al. (2000a) suggested that a line at $\sim 4430 \text{ \AA}$ on day 19 spectrum of SN 1993J may be Ba II $\lambda 4554$. But according to our spectral synthesis for SN 1996cb, it is undoubtedly Fe II feature (see day 7 spectrum shown in Figure 1).

To fit the 4610 \AA dip in the spectra of day 24 and 30 by C II $\lambda\lambda 4738, 4744$, we make C II to be detached at $v_{\min} = 9,800 \text{ km s}^{-1}$. However, from day 37 onwards, the feature formed in this way is too blue to fit the observed one. Inspecting these spectra closely, we find that this dip always attaches to the blueward edge of H_{β} absorption that it looks like a satellite line. We note that Baron et al. (2000) met the same problem of the lack of a strong candidate for the 4610 \AA feature when analyzing the spectra of Type II SN 1999em. By using a full NLTE code PHOENIX, they found that it is produced by complicated NLTE effects varying the Balmer level populations in the mid-velocity range. They named it and H_{β} together “double H_{β} ”. It is interesting to note that Utrobin, Chugai, & Adronova (1995) got a close idea, namely a radial dependence of Sobolev optical depth with two maxima, to explain the blue emission satellite of the famous “Bochum event” in SN 1987A. The recurrence of this phenomenon in these three otherwise quite different supernova arouses the question how generally it would exist.

Since SN 1987A (Williams 1987), Sc II and Sr II features are identified in many other Type II supernovae, e.g. SN 1992H (Clocchiatti et al. 1996), SN 1995V (Fassia et al. 1998), and SN 1997D (Turatto et al. 1998), and often coexist with Ba II ones. Can the $\sim 5500 \text{ \AA}$ bump here be identified as Sc II $\lambda 5527$, especially in the day 30 spectrum? We invoke Sc II in our synthesis calculations but find that the synthetic emission feature peaks at 5490 \AA , 20 \AA redder than the observed one on day 30, i.e. 5510 \AA . Furthermore, the Sc II $\lambda 4247$ is much too strong if the excitation temperature $\leq 12,000 \text{ K}$. As shown in Figure 1 (dotted line), Sr II $\lambda 4078$ blending with H_{δ} can fit the $\sim 4000 \text{ \AA}$ notch the same well as Ni II lines on day 10, but in the price of an unwanted absorption feature due to Sr II $\lambda 4215$.

5. Conclusion

We have analyzed the photospheric spectra of Type IIb SN 1996cb from day 7 to day 107 and made detailed line identifications by using the parameterized supernova synthetic-

spectrum code SYNOW. Our findings are the following:

1. The photospheric velocity evolves from $11,000 \text{ km s}^{-1}$ on day 7 to $3,000 \text{ km s}^{-1}$ on day 107, which makes some constraint on the explosion kinetic energy and ejecta mass, i.e. $E \approx 0.7 - 1.6 \times 10^{51} \text{ ergs} \cdot (M_{\text{ej}}/3M_{\odot})$.
2. The minimum velocity of hydrogen envelope is $v_{\text{min}}^{\text{HI}} \sim 9,500 - 10,500 \text{ km s}^{-1}$, corresponding to a mass of hydrogen envelope of $0.1 - 0.2 M_{\odot}$, smaller than that of SN 1993J.
3. Distinct Ni II and Co II features have been identified. The former is most likely primordially originated. The latter shows that newly synthesized radioactive elements has been mixed outward to at least $7,000 \text{ km s}^{-1}$, which favors a mass of helium core of the progenitor of $\lesssim 3.3 M_{\odot}$.
4. The bulk of the blueshift of [O I] $\lambda 5577$ net emission is attributed to line blending, although a still considerable residual $\sim 20 \text{ \AA}$ remains till the late phase. On the other hand, the superficial blueshift of He I $\lambda 5876$ peak can be fully explained as the blending effect with H_{α} .

Although the results presented in this paper are calculated with a parameterized code under the purely resonant scattering assumption, they may serve as initial references for detailed NLTE spectrum modeling, which is self-consistent and more reliable but on the other hand time-consuming. The modeling of the light curve of SN 1996cb, coupled with what have been derived from our direct spectral analysis, like the evolution of photospheric velocity, minimum velocity of hydrogen envelope and extent of ^{56}Ni mixing, is in progress.

We specially thank David Branch for providing us with the code SYNOW, and for helpful discussions. We are grateful to Ken'ichi Nomoto, Takayoshi Nakamura, Hideyuki Umeda, and Kazuhito Hatano for discussions. Jinsong Deng is currently supported by the JSPS Postdoctoral Fellowship for Foreign Researchers. This work has been supported by Grants-in-Aid for Scientific Research from JSPS and COE research (07CE2002) of the Japanese Ministry of Education, Science, Culture and Sports, and by Chinese Natural Science Foundation.

REFERENCES

- Baron, E., Hauschildt, P. H., & Branch, D. 1994, *ApJ*, 426, 334
- Baron, E., Hauschildt, P. H., Branch, D., et al. 1995, *ApJ*, 441, 170

- Baron, E., Branch, D., Hauschildt, .P. H., et al. 2000, ApJ, 545, 444
- Barbon, R., Benetti, S., Cappellaro, E., et al. 1995, A&AS, 110, 513
- Bartunov, O. S., Blinnikov, S. I., Pavlyuk, N. N., et al. 1994, A&A, 281, L53
- Benetti, S., Cappellaro, E., Turatto, M., et al. 2000, IAU Circ., 7375
- Bhatia, A. K., & Kastner, S. O. 1995, ApJ, 96, 325
- Blinnikov, S. I., Eastman, R., Bartunov, O. S., et al. 1998, ApJ, 496, 454
- Blinnikov, S. I., Lundqvist, P., Bartunov, O., et al. 2000, 532, 1132
- Branch, D. 1980, in Proc. Workshop on Atom. Phys. and Spectrsc., Supernovae Spectra, ed. R. Meyerott & G. H. Gillespie (New York: AIP), 39
- Chornock, R., Modjaz, M., & Filippenko, A. V. 2001, IAU Circ., 7618
- Clocchiatti, A., Benetti, S., Wheeler, J. C., et al. 1996, AJ, 111, 1286
- Deng, J. S., Qiu, Y. L., Hu, J. Y., et al. 2000, ApJ, 540, 452
- Duschinger, M., Puls, J., Branch, D., et al. 1995, A&A, 297, 802
- Eastman, R. G., & Kirshner, R. P., 1989, 347, 771
- Eastman, R. G., Schmidt, B. P., & Kirshner, R. 1996, ApJ, 466, 911
- Fassia, A., Meikle, W. P. S., Geballe, T. R., et al. 1998, MNRAS, 299, 150
- Filippenko, A. V. 1988, AJ, 96, 1941
- Filippenko, A. V., & Shields, J. C. 1989, IAU Circ., 4851
- Filippenko, A. V., Porter, A. C., & Sargent, W. L. W. 1990, AJ, 100, 1575
- Filippenko, A. V., Matheson T., Barth, A. J. 1994, ApJ, 108, 2220
- Filippenko, A. V. 1997, ARA&A, 35, 309
- Filippenko, A. V., & Chornock, R. 2001, IAU Circ., 7636
- Finn, R. A., Fesen, R. A., Darling, C. W., et al. 1995, ApJ, 110, 300
- Fisher, A. 2000, Ph.D. thesis, Univ. of Oklahoma

- Franson, C., Lundqvist, P., & Chevalier, R. A. 1996, *ApJ*, 461, 993
- Garnavich, P., & Kirshner, R. 1997, *IAU Circ.*, 6529
- Hachisu, I., Matsuda, T., Nomoto, K., et al. 1991, *ApJ*, 368, L27
- Harkness, R. P., Wheeler, J. C., Margon, B., et al. 1987, *ApJ*, 317, 355
- Hatano, K., Branch, D., Fisher, A., et al. 1999, *ApJS*, 121, 233
- Hatano, K., Branch, D., Fisher, A., et al. 1999, *ApJ*, 525, 881
- Houck, J. C., & Fransson, C. 1996, *ApJ*, 456, 811
- Höflich, P., Langer, N., & Duschinger, M. 1993 *A&A*, 275, L29
- Hill, G. C., et al. 1999, *IAU Circ.*, 7186
- Iwamoto, K., Young, T. R., Nakasato, N., et al. 1997, *ApJ*, 477, 865
- Jeffery, D. J., & Branch, D. 1990, in *Jerusalem Winter School for Theoretical Physics, Vol. 6, Supernovae*, ed. P. Ruiz-Lapuente, R. Canal, & J. Isern (Dordrecht: Kluwer), 659
- Kifonidis, K., Plewa, T., Janka, H. Th., et al. 2000, *ApJ*, 531, L123
- Kurucz, R. L. 1993, *Kurucz CD-ROM, Atomic Data for Opacity Calculations*
- Lewis, J. R., Walton, N. A., Meikle, W. P. S., et al. 1994, *MNRAS*, 266, L27
- Li, H., & McCray, R. 1992, *ApJ*, 387, 309
- Li, H., & McCray, R. 1993, *ApJ*, 405, 730
- Lucy, L. B 1991, *ApJ*, 383, 308
- Maeda, K., Nakamura T., Nomoto, K., et al. 2000, *ApJ*, submitted (astro-ph/0011003)
- Matheson, T., Filippenko, A. V., Barth, A. J., et al. 2000, *ApJ*, 120, 1487
- Matheson, T., Filippenko, A. V., Ho, L. C., et al. 2000, *ApJ*, 120, 1499
- Matheson, T., Filippenko A. V., Li, W. D., et al. 2001, *AJ*, 121, 1648
- Mazzali, P. A., Chugai, N., Turatto, M., et al. 1997, *MNRAS*, 284, 151
- Mazzali, P. A., Iwamoto, K., & Nomoto, K. 2000, *ApJ*, 545, 407

- Millard, J., Branch, D., Baron, E., et al. 1999, *ApJ*, 527, 746
- Nagataki, S., Shimizu, T. M., & Sato, K. 1998, *ApJ*, 495, 413
- Nakano, S., & Akoi, M. 1996, *IAU Circ.*, 6524
- Nomoto, K., Suzuki, T., Shigeyama, T., et al. 1993, *Nature*, 364, 507
- Nomoto, K., Iwamoto, K., & Suzuki, T. 1995, *Phys. Rep.*, 256, 173
- Olson, G. L. 1982, *ApJ*, 255, 267
- Prabhu, T. P., Mayya, Y. D., Singh, K. P., et al. 1995, *A&A*, 295, 403
- Podsiaklowski, Ph., Hsu, J. J. L., Joss, P. C., et al. 1993, *Nature*, 364, 509
- Rybicki, G. B., & Hummer, D. G. 1978, *ApJ*, 219, 654
- Saio, H., Kato, M., & Nomoto, K. 1988, *ApJ*, 331, 388
- Schlegel, D. J., Finkbeiner, D. P., & Davis, M. 1998, *ApJ*, 500, 525
- Shigeyama, T., Nomoto, K., Tsujimoto, T., et al. 1990, *ApJ*, 361, L23
- Shigeyama, T., Suzuki, T., Kumagai, S., et al. 1994, *ApJ*, 420, 341
- Sollerman, J., Leibundgut, B., & Spyromilio, J. 1998, *A&A*, 337, 207
- Spyromilio, T. 1994, *MNRAS*, 266, L61
- Swartz, D. A., Filippenko, A. V., Nomoto, K., et al. 1993, *ApJ*, 411, 313
- Swartz, D. A., Clocchiatti, A., Benjamin, R., et al. 1993, *Nature*, 365, 232
- Turatto, M., Mazzali, P. A., Young, T. R., et al. 1998, *ApJ*, 498, L129
- Patat, E., Chugai, N., & Mazzali, P. A. 1995, *A&A*, 299, 715
- Qiao, Q. Y., Li, W. D., Qiu, Y. L., et al. 1996, *IAU Circ.*, 6527
- Qiu, Y. L., Li, W. D., Qiao, Q. Y., et al. 1999, *AJ*, 117, 736
- Utrobin, V. 1994, *A&A*, 281, L89
- Utrobin, V., Chugai, N. N., & Adronova, A. A. 1995, *A&A*, 295, 129
- Utrobin, V. P. 1996, *A&A*, 306, 219

- Wang, L. F. & Hu, J. Y. 1994, *Nature*, 369, 380
- Wang, L., & Wheeler, J. C. 1996, *IAU Circ.*, 6351
- Wang, L., Howell, D. A., Höflich, P., et al. 2001, *ApJ*, 550, 1030
- Wheeler, J. C., & Filippenko, A. V. 1996, in *Supernova and Supernova Remnants*, ed. R. A. McCray & Z. Wang (Cambridge University Press), 241
- Whilliams, R. E. 1987, *ApJ*, 320, L117
- Woosley, S. E., Eastman, R. G., Weaver, T. A., et al. 1994, *ApJ*, 429, 300
- Young, T. R., Baron, E., & Branch, D. 1995, *ApJ*, 449, L51
- Zhang, Q., Hu, J. Y., Wang, L. F., et al. 1995, *MNRAS*, 277, 1115
- Zhang, Q., & Wang, Z. R. 1996, *A&A*, 307, 166

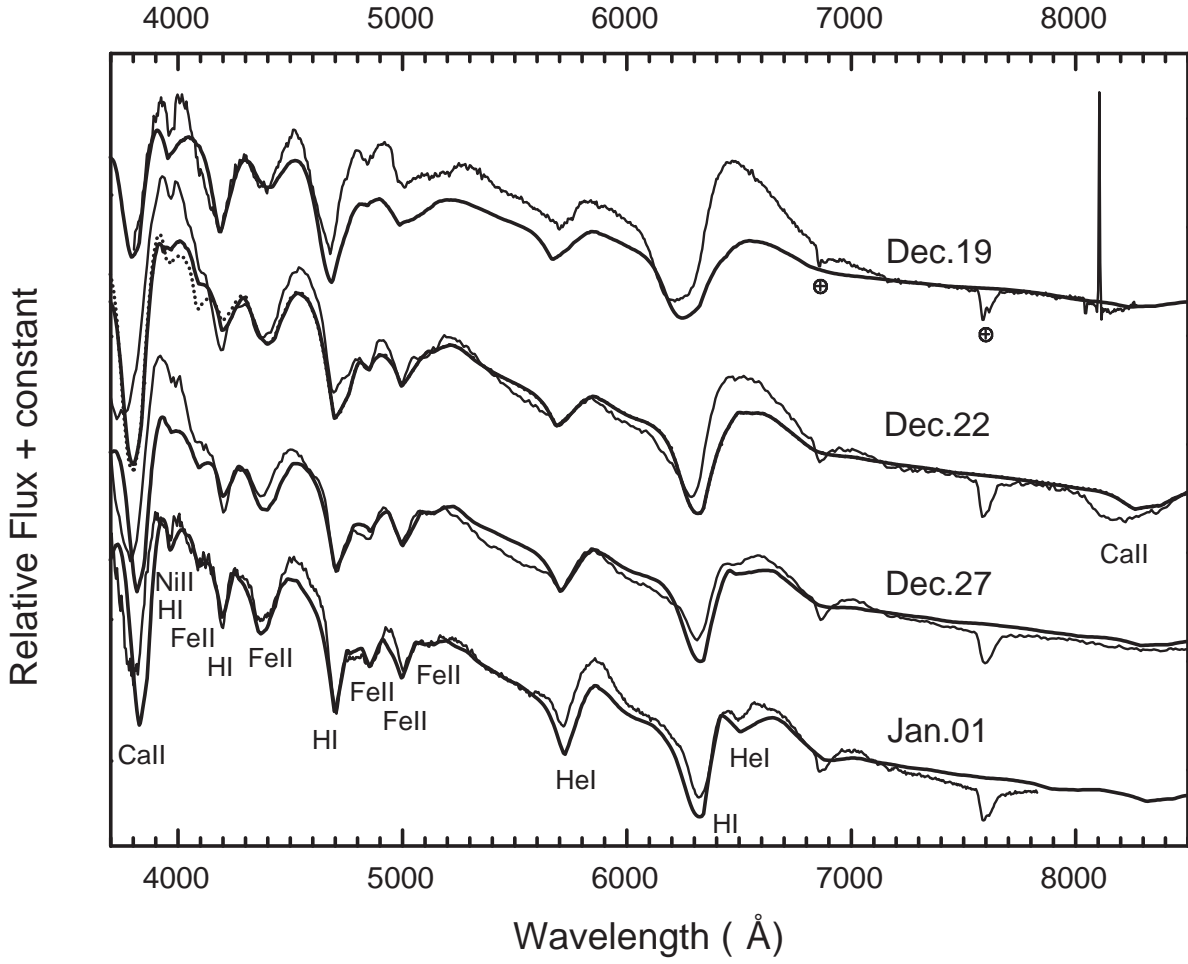


Fig. 1.— Observed spectra (thin solid lines) from day 7 to day 20 compared with best fit synthetic spectra (thick solid lines).

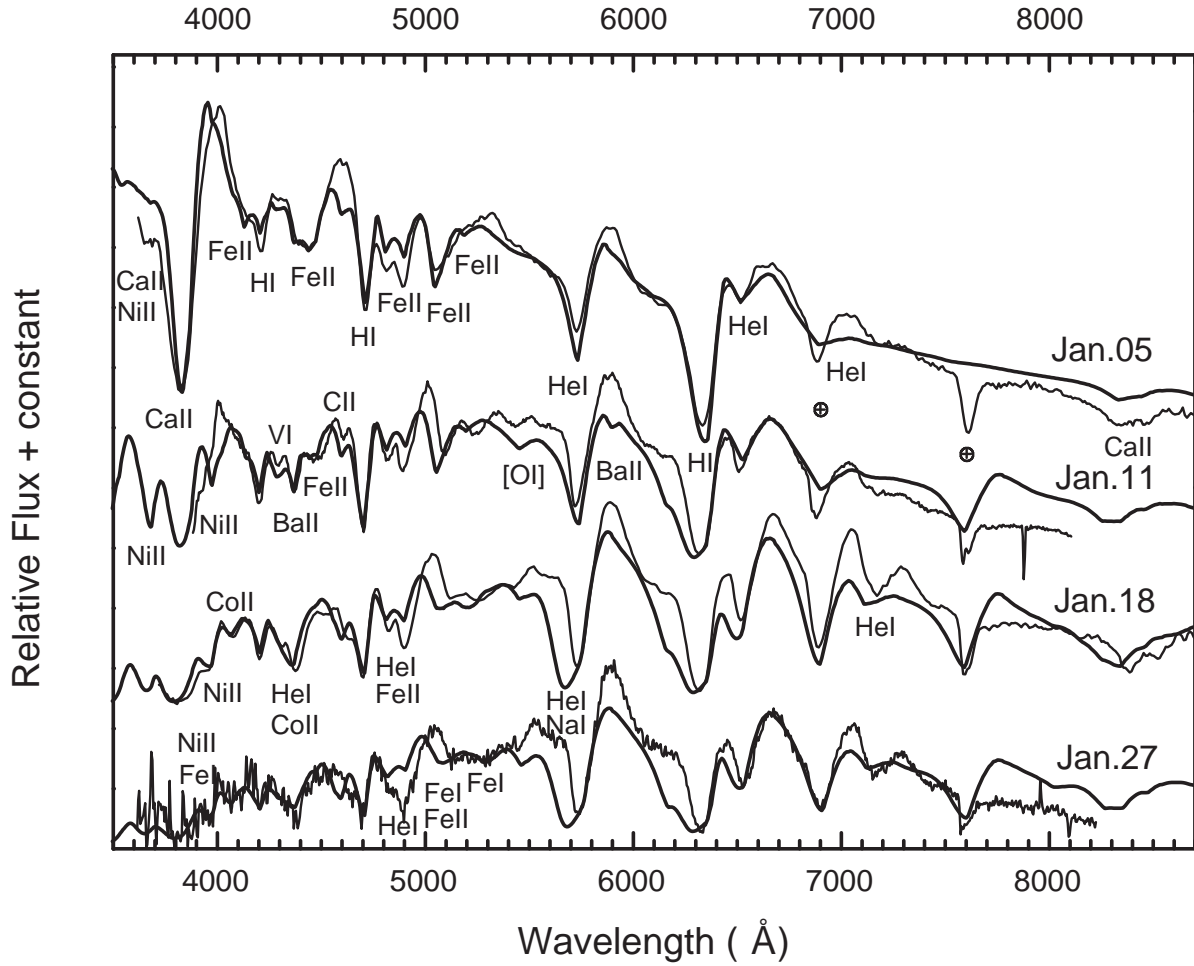


Fig. 2.— Observed spectra (thin solid lines) from day 21 to day 46 compared with best fit synthetic spectra (thick solid lines).

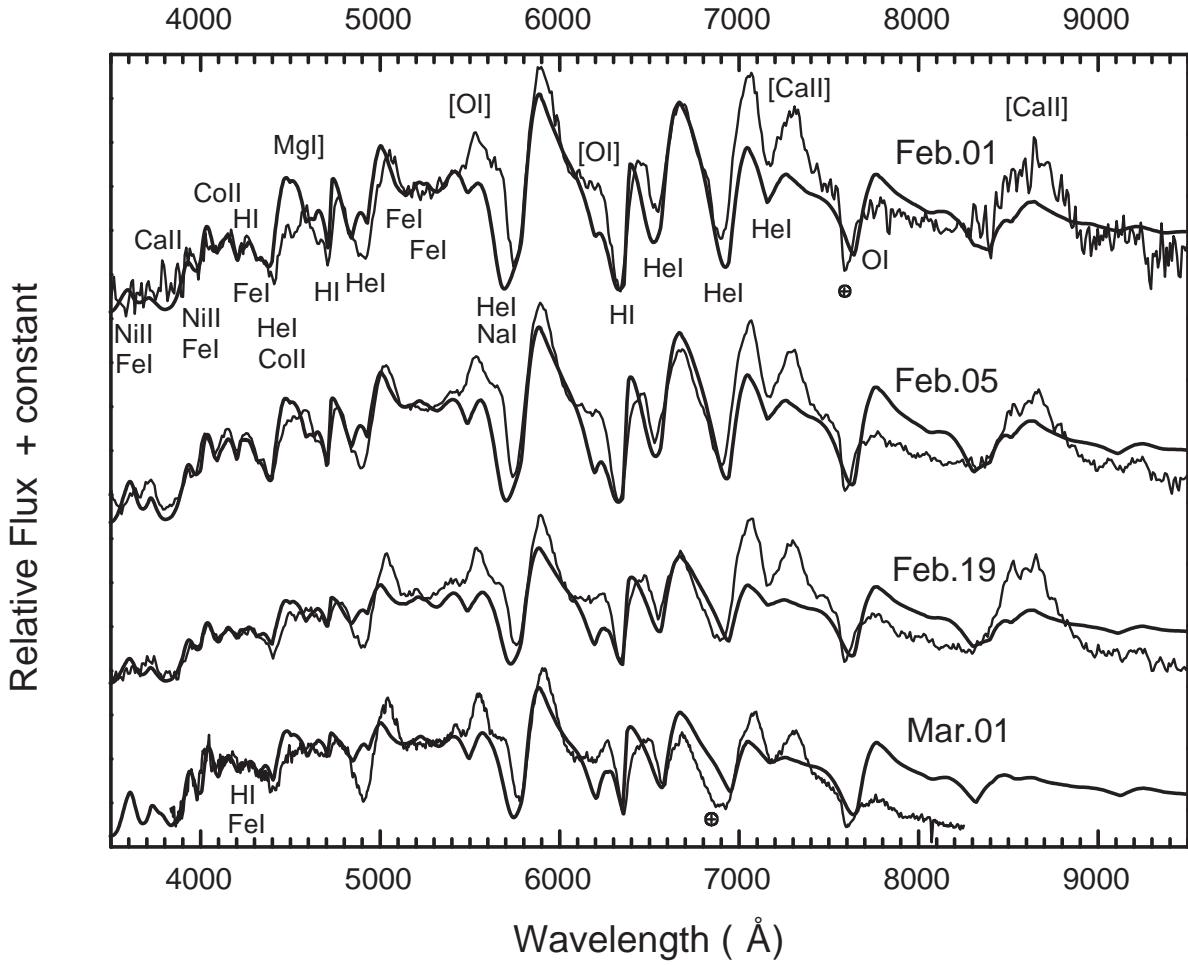


Fig. 3.— Observed spectra (thin solid lines) from day 51 to day 80 compared with best fit synthetic spectra (thick solid lines).

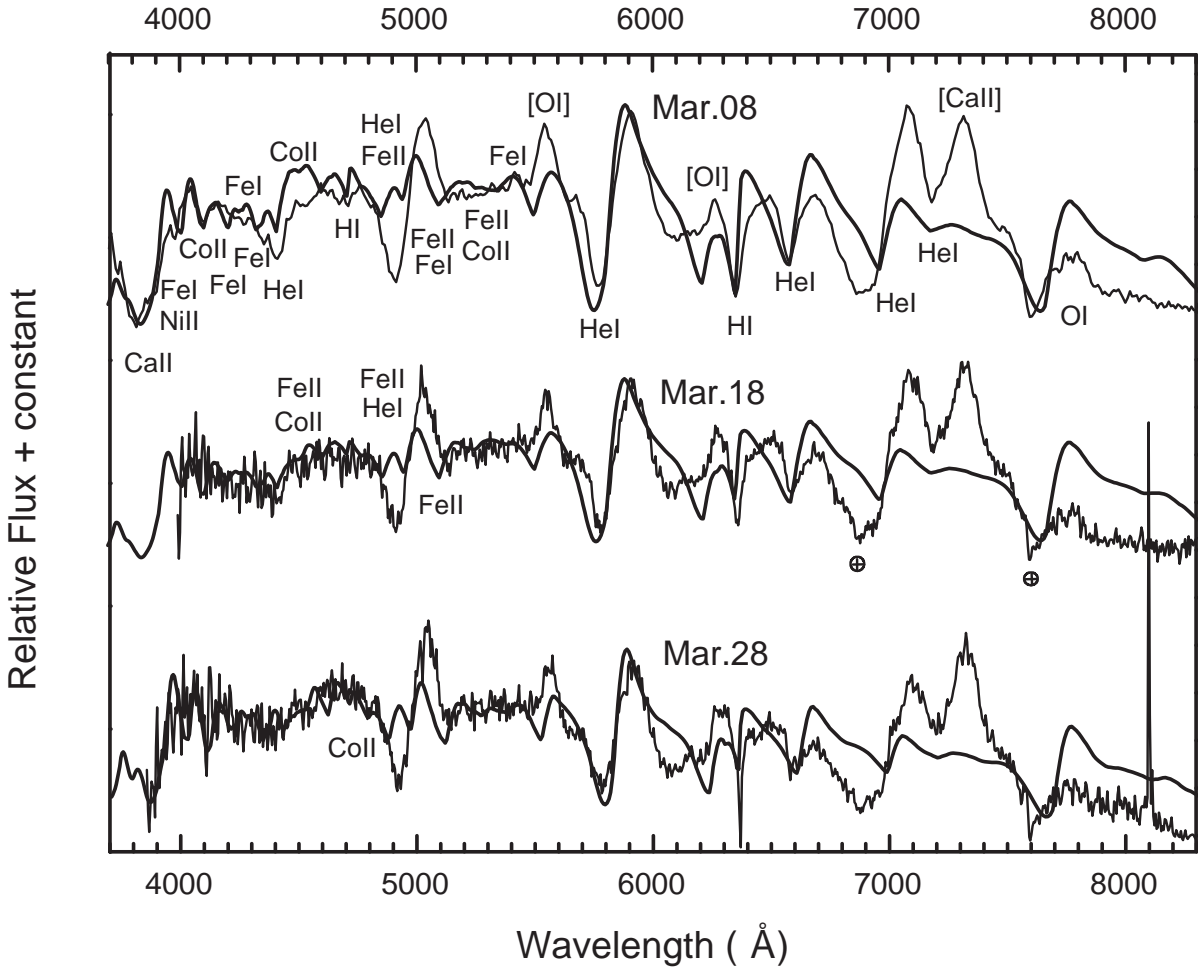


Fig. 4.— Observed spectra (thin solid lines) from day 87 to day 107 compared with best fit synthetic spectra (thick solid lines).

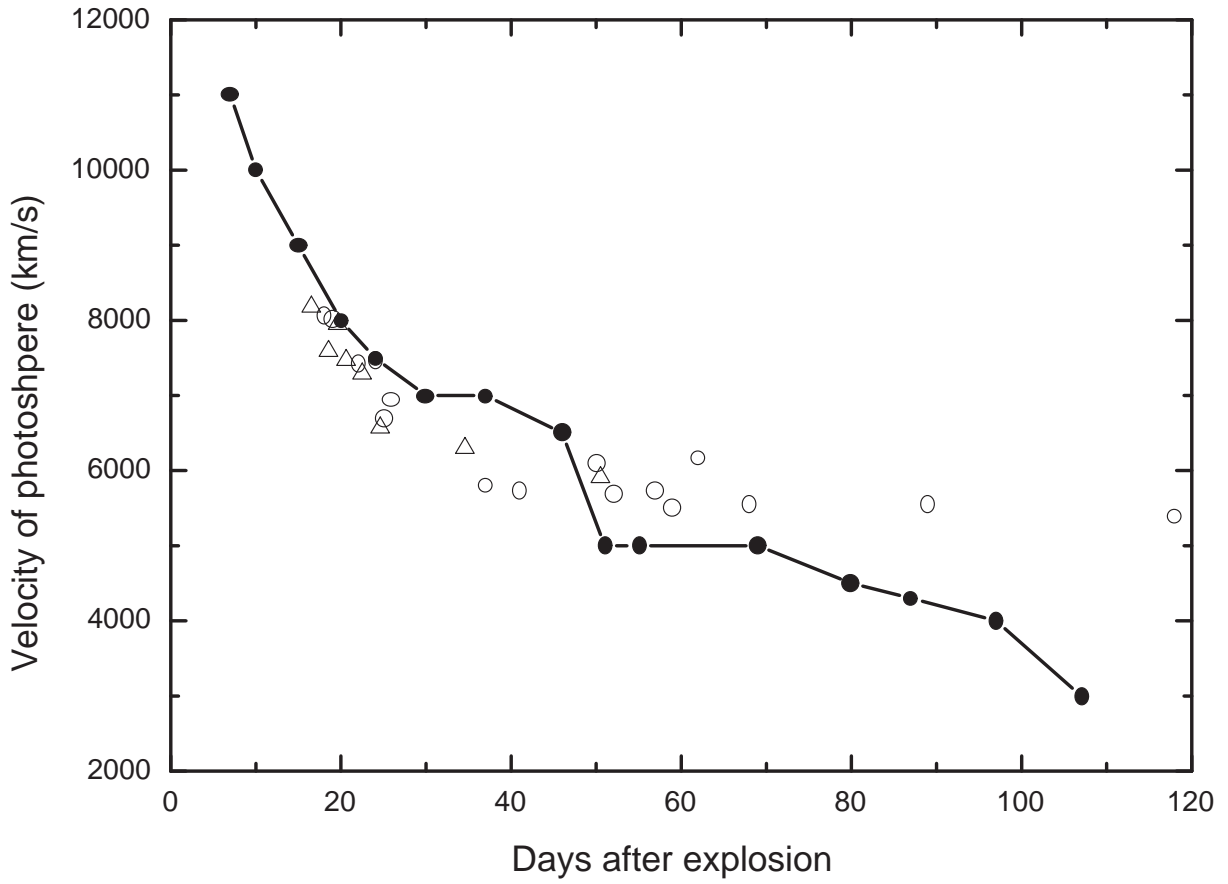


Fig. 5.— Photospheric velocities of SN 1996cb (filled circles) compared with those of SN 1993J measured by Prabhu et al. (1995, open triangles) and Barbon et al.(1995, open circles).

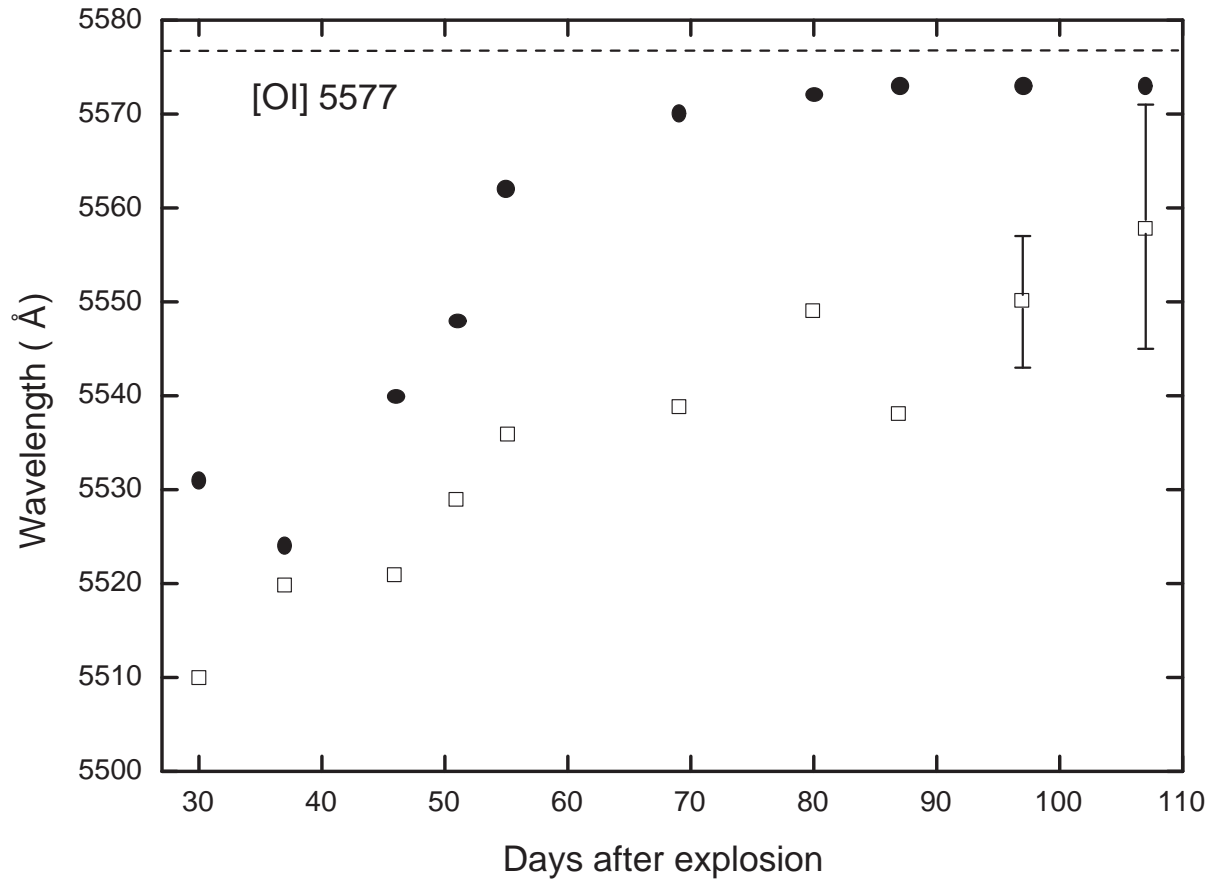


Fig. 6.— Peak wavelength of [O I] $\lambda 5577$ in observed spectra (open squares) compared with that in best fit synthetic spectra (filled circles).

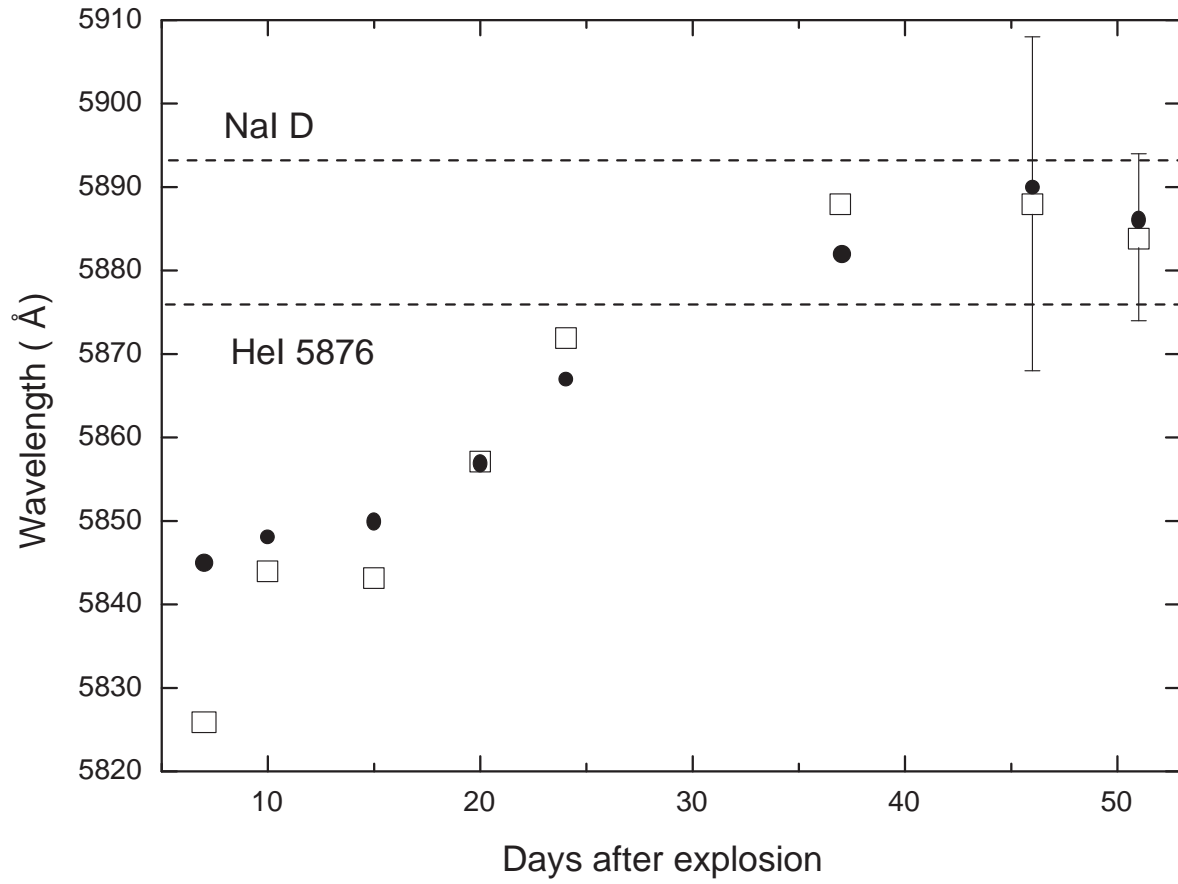


Fig. 7.— Peak wavelength of He I λ 5876 in observed spectra (open squares) compared with that in best fit synthetic spectra (filled circles).

Table 1. Epochs and fitting parameters of the observed spectra

Date(UT)	Epoch	v_{ph} (km s ⁻¹)	T_{bb} (K)
1996 Dec 19	7/-14	11,000	10,500
1996 Dec 22	10/-11	10,000	9,700
1996 Dec 27	15/-6	9,000	9,300
1997 Jan 1	20/-1	8,000	10,500
1997 Jan 5	24/+3	7,500	7,500
1997 Jan 11	30/+9	7,000	6,200
1997 Jan 18	37/+16	7,000	5,200
1997 Jan 27	46/+25	6,500	5,500
1997 Feb 1	51/+30	5,000	5,000
1997 Feb 5	55/+35	5,000	5,000
1997 Feb 19	69/+48	5,000	5,000
1997 Mar 1	80/+59	4,500	6,000
1997 Mar 8	87/+66	4,300	6,000
1997 Mar 18	97/+76	4,000	5,500
1997 Mar 28	107/+86	3,000	6,400